

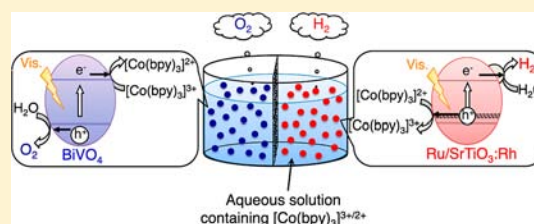
[Co(bpy)₃]^{3+/2+} and [Co(phen)₃]^{3+/2+} Electron Mediators for Overall Water Splitting under Sunlight Irradiation Using Z-Scheme Photocatalyst System

Yasuyoshi Sasaki, Hideki Kato,[†] and Akihiko Kudo*

Department of Applied Chemistry, Faculty of Science, Tokyo University of Science, 1-3 Kagurazaka, Shinjuku-ku, Tokyo 162-8601, Japan.

S Supporting Information

ABSTRACT: [Co(bpy)₃]^{3+/2+} and [Co(phen)₃]^{3+/2+} redox couples were revealed to play as electron mediators for Z-scheme photocatalyst systems composed of Ru/SrTiO₃:Rh and BiVO₄ powders for overall water splitting under visible light irradiation. These electron mediators were effective for only the combination of SrTiO₃:Rh with BiVO₄. They did not work when nondoped SrTiO₃ and TiO₂ of H₂-evolving photocatalysts and WO₃ of O₂-evolving photocatalysts were employed. These results indicated that the affinity between photocatalysts and the Co-complex electron mediators was important. The photocatalytic activity depended on pH. Neutral pH conditions gave the highest activity for overall water splitting. The Z-scheme photocatalyst system was also confirmed to split water under sunlight irradiation at the rates depending on weather. Moreover, overall water splitting by the Z-scheme photocatalyst system with the Co-complex electron mediator using a reaction cell in which the Ru/SrTiO₃:Rh suspension was divided from BiVO₄ suspension by a membrane filter resulted in H₂ evolution separated from that of O₂.



Overall water splitting by the present system steadily proceeded for a long time. The Z-scheme photocatalyst system was also confirmed to split water under sunlight irradiation at the rates depending on weather. Moreover, overall water splitting by the Z-scheme photocatalyst system with the Co-complex electron mediator using a reaction cell in which the Ru/SrTiO₃:Rh suspension was divided from BiVO₄ suspension by a membrane filter resulted in H₂ evolution separated from that of O₂.

1. INTRODUCTION

Overall water splitting by a semiconductor photocatalyst has been studied as one of the chemical methods for photon energy conversion.^{1–12} Most of the reported photocatalysts that are active for water splitting respond only to UV light due to their wide band gaps.^{1–5,9,10} Therefore, it is important to develop visible-light-driven photocatalysts to utilize sunlight efficiently. Domen et al. have reported that GaN–ZnO and ZnGeN₂–ZnO solid solutions are active photocatalysts for overall water splitting under visible light irradiation.^{6,11,12} However, there are only a limited number of powdered photocatalysts driven under sunlight irradiation.⁴

Some metal oxides,^{13–18} metal (oxy)sulfides,^{19–21} and metal (oxy)nitrides^{22,23} have been reported to show photocatalytic activities for sacrificial H₂ or O₂ evolution of the half reaction of overall water splitting under visible light irradiation, even if they are not active for overall water splitting. However, upon combining two kinds of photocatalysts for H₂ and O₂ evolution (denoted as H₂- and O₂-evolving photocatalysts, respectively) and a suitable electron mediator, water can be split into H₂ and O₂ in a stoichiometric amount through a two-step photoexcitation (Z-scheme) as shown in Figure 1.^{24–31} Sayama and Abe et al. have developed the Z-scheme systems composed of Pt/SrTiO₃:Cr,Ta¹⁵ and Pt/TaON²² of H₂-evolving photocatalysts, Pt/WO₃¹³ of an O₂-evolving photocatalyst, and an IO₃⁻/I⁻ electron mediator, succeeding in overall water splitting under visible light irradiation.^{25,26} It has also been realized that dye-sensitized Pt/H₄Nb₆O₁₇ could be utilized as a H₂-evolving photocatalyst.³⁰ We have also found that visible-light-driven Z-

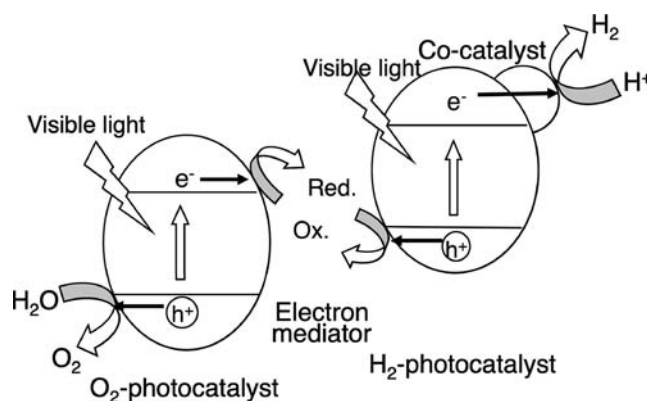


Figure 1. Overall water splitting using a Z-scheme photocatalyst system.

scheme systems composed of Pt- or Ru-loaded SrTiO₃:Rh¹⁶ of a H₂-evolving photocatalyst, BiVO₄,¹⁴ Bi₂MoO₆,¹⁷ and WO₃ of O₂-evolving photocatalysts, and an Fe³⁺/Fe²⁺ electron mediator can split water.^{28,30} Moreover, the Z-scheme photocatalyst systems driven by interparticle electron transfer without an electron mediator have been developed.³¹

Water splitting using powdered photocatalysts has a serious problem that the obtained gas is a mixture of H₂ and O₂. However, it would be possible to obtain H₂ separately from O₂

Received: January 9, 2013

Published: March 4, 2013

using electron mediators. Fujihara et al. have succeeded in overall water splitting under UV light irradiation by the Z-scheme photocatalyst system using two compartments that are connected by a Pt wire with a bromide ion and an iron ion as electron mediators.²⁴ Lee et al. also have reported that separate production is achieved by O₂ evolution on WO₃ from the filtered aqueous solution containing iron ions after H₂ evolution on Pt/SrTiO₃:Rh under visible light irradiation.³² Thus, not only photocatalyst materials but also electron mediators play an important role for Z-scheme photocatalyst systems. Therefore, it is important to find new electron mediators from the viewpoints of improvement of the efficiency of Z-scheme systems and development of new systems.

Many transition metal complexes have been reported as electron mediators in dye-sensitized solar cells.^{33–36} Grätzel et al. have found that the Co-complexes with imine-group ligands are comparable electron mediators to a well-known I₃⁻/I⁻ redox couple in the dye-sensitized solar cell.^{33,35} In addition, Elliot et al. have reported effective Co-complex mediators with other ligands.³⁴ There are some analogies between an electron mediator of the Z-scheme photocatalyst system and that of a dye-sensitized solar cell, for example, required redox potential, reversibility, and electron transfer between solid–liquid phases.

In the present study, we investigated the effectiveness of Co-complexes with 1,10-phenanthroline and 2,2'-bipyridine ligands as electron mediators for overall water splitting by Z-scheme photocatalyst systems. Solar water splitting and separated evolution of H₂ gas from O₂ gas were also demonstrated using the Z-scheme powdered photocatalyst systems.

2. EXPERIMENTAL SECTION

SrTiO₃,¹⁶ SrTiO₃:Rh(1%),¹⁶ SnNb₂O₆,³⁷ and TiO₂:Cr(2.3%),Sb(3.45%),³⁸ and BiVO₄¹⁴ powdered photocatalysts were prepared by a solid-state reaction or a liquid–solid-phase reaction as previously reported. The ratio of Sr/Ti/Rh in the SrTiO₃:Rh powder was 1.00–1.04/0.99/0.01. The obtained photocatalyst powders were confirmed to be desired phases by X-ray diffraction (Rigaku; MiniFlex). Surface areas of photocatalyst powders were determined by BET measurement (Coulter; SA3100). Commercial WO₃ (Nacalai Tesque; 99.5%) and anatase-phase TiO₂ (Merck; 99%) were used as received. Ru (0.7 wt %) and Pt (0.3 wt %) cocatalysts working as active sites for H₂ evolution were loaded on photocatalysts by photodeposition from aqueous methanol solutions (10 vol %) containing RuCl₃·nH₂O (Wako Pure Chemical; 99.9%) and H₂PtCl₆ (Tanaka Kikinzoku; 37.55% as Pt) as reported previously.²⁹ The cocatalyst-loaded photocatalysts were collected by filtration and washed with water.

[Co(bpy)₃]SO₄ and [Co(phen)₃]Cl₂ were synthesized by mixing the stoichiometric amounts of CoSO₄·7H₂O (Kanto Chemical; 99.0%) and 2,2'-bipyridine (Kanto Chemical; 99.0%) or 1,10-phenanthroline (Kanto Chemical; 99.0%), according to the literature.^{39,40} [Co(bpy)₃]SO₄ precipitation was obtained by mixing an aqueous CoSO₄ solution with 2,2'-bipyridine dissolved in ethanol solution. For [Co(phen)₃]Cl₂ preparation, an aqueous CoSO₄ solution was mixed with 1,10-phenanthroline dissolved in ethanol solution. A concentrated aqueous NaCl (Kanto Chemical; 99.9%) solution was added into the resulting Co-complex solution in order to precipitate [Co(phen)₃]Cl₂. The obtained Co-complex was recrystallized for removing impurities. The obtained compounds were confirmed to be desired Co-complexes by a UV–vis spectrometer (Jasco; UbestV-570).^{40,41}

The redox properties of these Co-complexes were measured by a potentiostat (Hokuto Denko; HAG3001). On the electrochemical measurement, Pt plates (1 cm²) were used as working and counterelectrodes. Ag | AgCl | KCl (sat., aq) was used as a reference electrode. Electrolytes of aqueous solutions dissolving the Co-complex (50 mmol L⁻¹) and K₂SO₄ (1 mmol L⁻¹) were purged with N₂ gas before measurements.

Photocatalytic reactions were mainly carried out in a Pyrex glass cell with a top window connected to a gas-closed system. For Z-schematic water splitting, H₂- and O₂-evolving photocatalyst powders (0.1 g each) were suspended by a magnetic stirrer in the aqueous [Co(bpy)₃]SO₄ or [Co(phen)₃]Cl₂ solution (120 mL) adjusted to the desired pH with H₂SO₄ or NaOH. Sacrificial H₂ and O₂ evolutions of half reactions of water splitting were also evaluated. [Co(bpy)₃]²⁺ and [Co(phen)₃]²⁺ were used for H₂ evolution as sacrificial reagents, while [Co(bpy)₃]³⁺ and [Co(phen)₃]³⁺ were employed for O₂ evolution. Trivalent Co-complexes of [Co(bpy)₃]³⁺ and [Co(phen)₃]³⁺ were prepared by photocatalytic oxidation of [Co(bpy)₃]²⁺ and [Co(phen)₃]²⁺ using Ru/SrTiO₃:Rh. The reactant solution was kept at 293 K. Ar gas at 40 Torr was introduced into the gas-closed system after deaeration. The suspension of the photocatalysts was irradiated with light using a 300-W Xe-arc lamp (Perkin Elmer; Cermax-PE300BF) or noncollective sunlight (October in Tokyo). Visible light (λ > 420 nm) was obtained by a cutoff filter (HOYA; L42). The amounts of evolved H₂ and O₂ were determined using an online gas chromatograph (Shimadzu; GC-8A, MS-5A column, TCD, Ar carrier).

Apparent quantum yields of a Z-scheme system (a two-photon excitation process) were determined by eq 1.

$$\begin{aligned} \text{apparent quantum yield (\%)} &= 100 \times \left[\frac{\text{the number of reacted electrons or holes}}{\text{the number of incident photons}} \right] \\ &= 100 \times \left[\frac{\text{the number of evolved O}_2 \text{ molecules} \times 8}{\text{the number of incident photons}} \right] \end{aligned} \quad (1)$$

The monochromatic light was obtained with band-pass filters and cutoff filters attached with a 300-W Xe-arc lamp. The photon flux of the monochromatic light was measured by a silicon photodiode (OPHIR; PD300-UV of a head and NOVA of a power monitor). A solar energy conversion was also determined by eq 2 using a solar simulator with an AM-1.5 filter (Yamashita Denso; YSS-80QA, 100 mW cm⁻²).

$$\begin{aligned} \text{solar energy conversion efficiency (\%)} &= 100 \times \left[\frac{\text{output energy as H}_2 / \text{J s}^{-1}}{[\text{energy dens. of incident solar light} / \text{W cm}^{-2}] \times [\text{irrad. area} / \text{cm}^2]} \right] \\ &= 100 \times \left[\frac{\text{std. Gibbs free energy of water, } \Delta G_{298}^0 / \text{J mol}^{-1}}{3600 \times [\text{energy dens. of incident solar light} / \text{W cm}^{-2}] \times [\text{irrad. area} / \text{cm}^2]} \right] \times \left[\frac{\text{rate of H}_2 \text{ evolution} / \text{mol h}^{-1}}{1} \right] \end{aligned} \quad (2)$$

3. RESULTS AND DISCUSSION

3.1. Development of Z-Scheme Photocatalyst Systems Employing Co-Complex Electron Mediators. Table 1 presents H₂ evolution on various H₂-evolving photocatalysts from aqueous solutions containing [Co(bpy)₃]²⁺, [Co(phen)₃]²⁺, and Co²⁺ ions. This H₂ evolution corresponds to the half reaction of the Z-schematic overall water splitting shown in Figure 1. The well-known Pt/TiO₂ and Pt/SrTiO₃ photocatalysts showed negligible activity in the present conditions (entries 1–4). The visible-light-driven Pt/SnNb₂O₆ photocatalyst that can produce H₂ in the presence of methanol also showed no activity (entries 5, 6). In contrast, Pt- or Ru-loaded SrTiO₃:Rh photocatalysts produced H₂ under visible light irradiation (entries 7–10). Importantly, the activity in the presence of Co²⁺ ions was negligible (entry 11), meaning

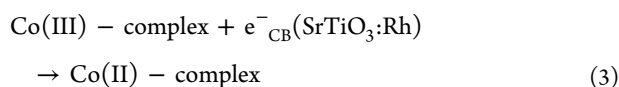
Table 1. H₂ Evolution from Aqueous Solutions Containing [Co(bpy)₃]²⁺, [Co(phen)₃]²⁺, and Co²⁺ Ions on Various Photocatalysts^a

entry	photocatalyst	electron donor	incident light /nm	init. activity / μmol h ⁻¹
1	Pt (0.3 wt %)/TiO ₂ -anatase	[Co(bpy) ₃] ²⁺	>300	0
2	Pt (0.3 wt %)/TiO ₂ -anatase	[Co(phen) ₃] ²⁺	>300	0.2
3	Pt (0.3 wt %)/SrTiO ₃	[Co(bpy) ₃] ²⁺	>300	0.02
4	Pt (0.3 wt %)/SrTiO ₃	[Co(phen) ₃] ²⁺	>300	0
5	Pt (0.3 wt %)/SnNb ₂ O ₆	[Co(bpy) ₃] ²⁺	>420	0
6	Pt (0.3 wt %)/SnNb ₂ O ₆	[Co(phen) ₃] ²⁺	>420	0
7	Pt (0.3 wt %)/SrTiO ₃ :Rh	[Co(bpy) ₃] ²⁺	>420	12
8	Pt (0.3 wt %)/SrTiO ₃ :Rh	[Co(phen) ₃] ²⁺	>420	9.5
9	Ru (0.7 wt %)/SrTiO ₃ :Rh	[Co(bpy) ₃] ²⁺	>420	16
10	Ru (0.7 wt %)/SrTiO ₃ :Rh	[Co(phen) ₃] ²⁺	>420	12
11	Ru (0.7 wt %)/SrTiO ₃ :Rh	Co ²⁺	>420	0.5

^aReaction conditions: catalyst, 0.1 g; starting reactant solution, 120 mL of aqueous [Co(bpy)₃]²⁺SO₄ or [Co(phen)₃]²⁺Cl₂ solution (0.5 mmol L⁻¹, initial pH: ~7); light source, a 300-W Xe-arc lamp; cell, top-irradiation cell with a Pyrex glass window. SrTiO₃:Rh powder was prepared by calcination at 1273 K without Sr excess.

that the activity of H₂ production is mainly due to Co-complex ions not due to Co²⁺ ions liberated from the Co-complex. Moreover, the Rh species doped in SrTiO₃:Rh was a key factor for H₂ evolution in the presence of these Co-complexes, judging from no activity on the nondoped SrTiO₃. In other words, the Rh species doped into the SrTiO₃ contributed not only to the formation of the electron donor level in the forbidden band for visible light response¹⁶ but also to the construction of the active site for oxidation of [Co(bpy)₃]²⁺ and [Co(phen)₃]²⁺ ions.

To clarify that this H₂ evolution proceeded accompanied with consumption of Co-complexes, the profile of time course of the H₂ evolution was studied, as shown in Figure S1 (Supporting Information [SI]). H₂ evolution on Pt- or Ru-loaded SrTiO₃:Rh stopped, when the amount of evolved H₂ reached close to the calculated amount of H₂ by assuming that all dissolved [Co(bpy)₃]²⁺ and [Co(phen)₃]²⁺ ions were oxidized to [Co(phen)₃]³⁺ and [Co(bpy)₃]³⁺ ions. Thus, [Co(bpy)₃]²⁺ and [Co(phen)₃]²⁺ ions in the reactant solution were completely consumed becoming [Co(bpy)₃]³⁺ and [Co(phen)₃]³⁺ ions after photocatalytic H₂ evolution over Ru/SrTiO₃:Rh. This was also supported by absorption spectra of the reactant solution after the photocatalytic reactions. Moreover, these results indicate that the backward reactions shown in the eq 3 did not proceed on the Pt- or Ru-loaded SrTiO₃:Rh photocatalyst.



This is an important character to construct a Z-scheme photocatalyst system.

Table 2 presents the activities for overall water splitting using Z-scheme systems composed of Ru/SrTiO₃:Rh of a H₂-

Table 2. Overall Water Splitting by the (Ru/SrTiO₃:Rh)-(O₂-Evolving Photocatalyst) Systems with [Co(bpy)₃]^{3+/2+} and [Co(phen)₃]^{3+/2+} Electron Mediators under Visible Light Irradiation^a

entry	O ₂ -evolving photocatalyst	starting reactant soln	activity / μmol h ⁻¹	
			H ₂	O ₂
1	WO ₃	[Co(bpy) ₃] ³⁺ SO ₄	14	0.5
2	WO ₃	[Co(phen) ₃] ³⁺ Cl ₂	15	0.4
3	TiO ₂ :Cr,Sb	[Co(bpy) ₃] ³⁺ SO ₄	3.0	0.8
4	TiO ₂ :Cr,Sb	[Co(phen) ₃] ³⁺ Cl ₂	1.3	0.7
5	BiVO ₄	[Co(bpy) ₃] ³⁺ SO ₄	10	4.8
6	BiVO ₄	[Co(phen) ₃] ³⁺ Cl ₂	7.9	3.5
7	BiVO ₄	CoSO ₄	1.0	0.2
8	BiVO ₄	2,2'-bipyridine	3.2	0.6
9	BiVO ₄	1,10-phenanthroline	5.5	0.5

^aReaction conditions: catalyst, 0.1 g each; starting reactant solution, 120 mL of aqueous [Co(bpy)₃]³⁺SO₄ or [Co(phen)₃]³⁺Cl₂ solution (1 mmol L⁻¹, initial pH: 7); light source, a 300-W Xe-arc lamp with a cutoff filter (λ > 420 nm); cell, top-irradiation type. SrTiO₃:Rh power was prepared by calcination at 1273 K without Sr excess.

evolving photocatalyst and various visible-light-driven O₂-evolving photocatalysts. Here, the Ru cocatalyst loaded by photodeposition was employed, because no backward reaction (H₂ + O₂ → 2 H₂O) proceeded on the Ru cocatalyst, unlike the Pt cocatalyst.²⁹ The tris(bipyridyl)cobalt(II,III) complex system employing BiVO₄ and the tris(phenanthroline)cobalt(II,III) complex systems employing TiO₂:Cr,Sb and BiVO₄ split water into H₂ and O₂ in a stoichiometric amount (entries 4–6). In contrast, only H₂ evolved, when WO₃ was employed (entries 1 and 2, and Figure S2 (SI)). This different behavior depending on the kind of O₂-evolving photocatalyst can be explained by the potential of photogenerated holes. Holes are photogenerated in the valence bands consisting of O2p for WO₃ and Bi6s for BiVO₄, and in the impurity level formed by Cr³⁺ for TiO₂:Cr,Sb. Holes photogenerated in the valence band consisting of O2p possess stronger oxidation power than those of Bi6s and Cr³⁺, resulting in oxidative decomposition of the Co-complex on WO₃ rather than just oxidation of Co(II)-complexes to Co(III)-complexes. To clarify if Co-complexes themselves work as an electron mediator, CoSO₄, 2,2'-bipyridine, and 1,10-phenanthroline were added into the reactant solution (entries 7–9). Water splitting did not proceed in the presence of any additives, and H₂ mainly evolved in the presence of CoSO₄, 2,2'-bipyridine, and 1,10-phenanthroline. These results clearly indicate that [Co(bpy)₃]^{3+/2+} and [Co(phen)₃]^{3+/2+} redox couples worked effectively as electron mediators in the Z-scheme system consisting of Rh/SrTiO₃:Rh and BiVO₄. Figure 2 shows time courses of overall water splitting using the (Ru/SrTiO₃:Rh)-(BiVO₄) systems with [Co(bpy)₃]^{3+/2+} and [Co(phen)₃]^{3+/2+} electron mediators under visible light irradiation. Both photocatalyst systems steadily split water for a long time. The activity of the [Co(bpy)₃]^{3+/2+} electron mediator system was higher than that of the [Co(phen)₃]^{3+/2+} electron mediator system. The turnover numbers of reacted electrons to the [Co(bpy)₃]^{3+/2+} and [Co(phen)₃]^{3+/2+} were 35 and 25, respectively, indicating good stability of both Co-complexes as an electron mediator.

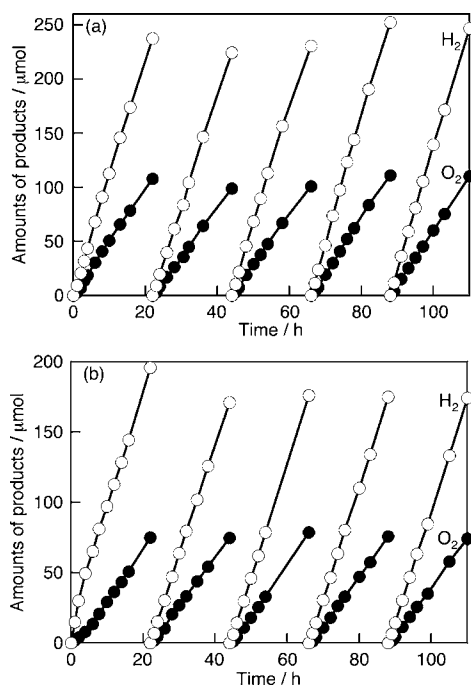


Figure 2. Overall water splitting under visible light irradiation by (Ru/SrTiO₃:Rh)–(BiVO₄) systems employing (a) [Co(bpy)₃]^{3+/2+} and (b) [Co(phen)₃]^{3+/2+} electron mediators. Reaction conditions: catalyst, 0.1 g each; starting reactant solution, 120 mL of aqueous (a) [Co(bpy)₃]^{3+/2+}SO₄ and (b) [Co(phen)₃]^{3+/2+}Cl₂ solutions (0.5 mmol L⁻¹, initial pH: ~7); light source, a 300 W Xe-arc lamp with a cutoff filter ($\lambda > 420$ nm); cell, top-irradiation type. SrTiO₃:Rh was prepared by calcination at 1273 K without Sr excess.

The authors have previously reported that excess Na in the preparation of a NaTaO₃ photocatalyst improved its activity.^{3,5} Therefore, the authors investigated the effect of excess Sr and calcination temperature in the preparation of the SrTiO₃:Rh photocatalyst on the activity for overall water splitting over the Z-scheme system employing BiVO₄ and the [Co(bpy)₃]^{3+/2+} electron mediator as shown in Table 3. The initial pH of the reactant solution was adjusted to 3.8 with H₂SO₄ for all reactions. SrTiO₃:Rh prepared with excess Sr was almost a single phase of perovskite structure as shown in Figure S3 (SI). All Z-scheme systems employing SrTiO₃:Rh prepared with excess Sr showed higher activities for overall water splitting than that of SrTiO₃:Rh without excess Sr. Moreover, the activity also depended on calcination temperature in the preparation of SrTiO₃:Rh. The highest activity was obtained, when calcined at 1373 K with 3% excess of Sr (entries 5–8). Comparing with the system employing an Fe³⁺/Fe²⁺ electron mediator, the activity was more than double (entries 7 and 10). Moreover, overall water splitting by the optimized Z-scheme system with the Co-complex steadily proceeded for 17 h as shown in Figure 3. The turnover number of reacted electrons to the [Co(bpy)₃]^{3+/2+} electron mediator was 56. The apparent quantum efficiency of the Z-scheme system was 2.1% at 420 nm. Thus, new and highly active visible-light-driven Z-scheme photocatalyst systems for water splitting were successfully developed.

3.2. Solar Water Splitting Using the Z-Scheme Photocatalyst System Employing the Co-Complex Electron Mediator. Water splitting under real sunlight by the (Ru/SrTiO₃:Rh)–(BiVO₄)–([Co(bpy)₃]^{3+/2+}) system was demonstrated in Tokyo, as shown in Figure 4. The amounts of

Table 3. Effects of Ratio of Sr to (Ti + Rh) and Calcination Temperature in the Preparation of SrTiO₃:Rh on Overall Water Splitting by a (Ru/SrTiO₃:Rh)–(BiVO₄)–([Co(bpy)₃]^{3+/2+}) System^a

entry	Sr:(Ti + Rh) ratio	calcination temperature /K	surface area /m ² g ⁻¹	activity / $\mu\text{mol h}^{-1}$	
				H ₂	O ₂
1	1.00	1273	2.8	13	5.8
2	1.01	1373	2.6	32	14
3	1.02	1273	3.1	69	35
4	1.02	1373	2.7	91	41
5	1.03	1273	3.3	66	32
6	1.03	1323	3.0	80	35
7	1.03	1373	2.7	100	47
8	1.03	1473	2.2	64	29
9	1.04	1273	3.2	63	28
10	1.03	1373	2.7	43 ^b	21 ^b

^aReaction conditions: catalyst, 0.1 g each; starting reactant solution, 120 mL of an aqueous [Co(bpy)₃]^{3+/2+}SO₄ solution (0.5 mmol L⁻¹, initial pH: 3.8); light source, a 300-W Xe-arc lamp with a cutoff filter ($\lambda > 420$ nm); cell, top-irradiation type. ^bAqueous FeCl₃ solution (2 mmol L⁻¹, pH 2.4).

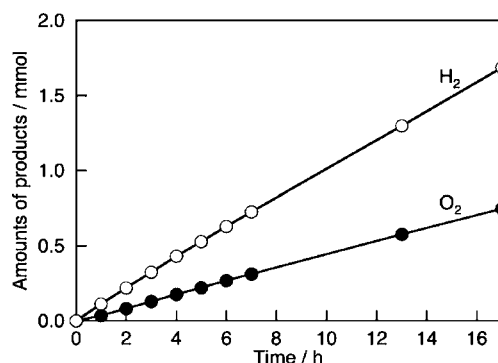


Figure 3. Overall water splitting by a (Ru/SrTiO₃:Rh)–(BiVO₄)–([Co(bpy)₃]^{3+/2+}) system under visible light irradiation. Reaction conditions: catalyst, 0.1 g each; starting reactant solution, 120 mL of an aqueous [Co(bpy)₃]^{3+/2+}SO₄ solution (0.5 mmol L⁻¹, initial pH: 3.8); light source, a 300 W Xe-arc lamp with a cutoff filter ($\lambda > 420$ nm); cell, top-irradiation type. SrTiO₃:Rh powder was prepared by calcination at 1373 K with Sr 3% excess.

evolved H₂ and O₂ for 2 h on sunny day (28th 9–11 and 11:30–13:30) were about 260 and 110 μmol , respectively. In contrast, the amounts of these gases on a cloudy day were almost half. The solar energy conversion efficiency of the present Z-scheme system was determined to be 0.06% using a solar simulator (AM-1.5, 100 mW cm⁻²). Thus, the Z-scheme photocatalyst system employing the Co-complex electron mediator was confirmed to be active for solar water splitting.

3-3. Separate Evolution of H₂ and O₂ by Water Splitting Using Powdered Photocatalysts. In general, the mixed gas of H₂ and O₂ is obtained in overall water splitting using a powdered photocatalyst. This will be the serious problem of a powdered photocatalyst for practical use. However, a Z-scheme photocatalyst system can overcome this issue, because it can produce H₂ separately from O₂. Therefore, we investigated H₂ evolution separated from O₂ by water splitting using the Z-scheme photocatalyst system with the [Co(bpy)₃]^{3+/2+} electron mediator. A Ru/SrTiO₃:Rh-s-

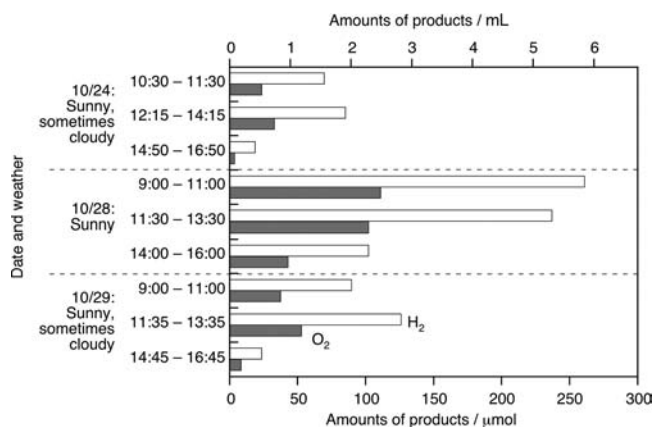


Figure 4. Solar water splitting by a (Ru/SrTiO₃:Rh)–(BiVO₄)–([Co(bpy)₃]^{3+/2+}) system. Reaction conditions: catalyst, 0.1 g each; starting reactant solution, 150 mL of an aqueous [Co(bpy)₃]SO₄ solution (0.2 mmol L⁻¹, initial pH: 3.8); light source, sunlight in autumn in Tokyo; irradiated area, 33 cm². SrTiO₃:Rh was prepared with Sr 3% excess and calcination at 1373 K.

pendent compartment for H₂ evolution was separated from a BiVO₄-suspended compartment for O₂ evolution by a membrane filter with a pore size of 10 μm as shown in Figure 5a. Figure 5b shows overall water splitting using the two-compartment-reactor under visible light irradiation. H₂ steadily evolved in the Ru/SrTiO₃:Rh-suspended compartment at the rate of 110 μL h⁻¹ after 3 h, while O₂ and a small amount of H₂ were detected in the BiVO₄-suspended compartment at the rates of 43 and 4.3 μL h⁻¹, respectively. The H₂ detected in the BiVO₄-suspended compartment was contaminated from the Ru/SrTiO₃:Rh-suspended compartment, because H₂ molecule can easily pass through the membrane filter. In the absence of the [Co(bpy)₃]^{3+/2+} electron mediator, no gases were detected with this separate system, indicating that the [Co(bpy)₃]^{3+/2+} redox couple assisted the electron transfer by shuttling between two compartments. In other words, water splitting proceeded in spite of separation of Ru/SrTiO₃:Rh from BiVO₄ powder, as long as the Co-complex electron mediator can travel back and forth between H₂- and O₂-evolving photocatalysts. Thus, separated evolution of H₂ from O₂ by water splitting under visible light irradiation was achieved using a powdered photocatalyst system.

3.4. Behavior of the Co-Complex As an Electron Mediator in the Z-Scheme Photocatalyst System. Behavior of [Co(bpy)₃]^{3+/2+} and [Co(phen)₃]^{3+/2+} redox couples as electron mediators during the photocatalytic reaction was studied in detail. Figure 6 shows absorption spectra of aqueous [Co(phen)₃]Cl₂ solutions as-prepared, after H₂ evolution on Ru/SrTiO₃:Rh (entry 8 in Table 1), and after overall water splitting by the (Ru/SrTiO₃:Rh)–(BiVO₄) system (entry 6 in Table 2). The absorption spectra of the aqueous solutions as-prepared (Figure 6a) and after H₂ evolution (Figure 6b) were assigned to [Co(phen)₃]²⁺ and [Co(phen)₃]³⁺ ions, respectively, as previously reported.^{40,41} In addition, we also confirmed that all dissolved [Co(phen)₃]²⁺ ions in the starting reactant solution were oxidized to [Co(phen)₃]³⁺ ions during H₂ evolution; the number of electrons used for H₂ evolution agreed well with that of [Co(phen)₃]²⁺, as shown in Figure S1 (SI). These results clearly indicate that H₂ evolved over Ru/SrTiO₃:Rh under

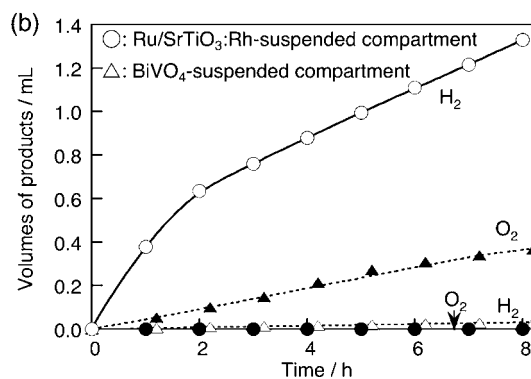
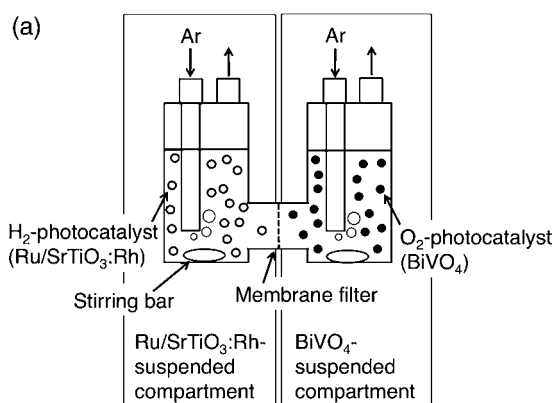


Figure 5. (a) Two-compartment-reactor for H₂ evolution separated from O₂ evolution. (b) H₂ evolution separated from O₂ evolution for overall water splitting by a (Ru/SrTiO₃:Rh)–(BiVO₄)–([Co(bpy)₃]^{3+/2+}) system. Catalyst: 0.1 g (Ru/SrTiO₃:Rh), 0.3 g (BiVO₄), starting reactant solution: 0.5 mmol L⁻¹ of an aqueous [Co(bpy)₃]SO₄ solution, 300 mL, initial pH adjusted to 3.8, light source: two 300 W Xe-arc lamps with cutoff filters (λ > 420 nm). SrTiO₃:Rh powder was prepared by calcination at 1373 K with Sr 3% excess. Open and close marks indicate H₂ and O₂, respectively.

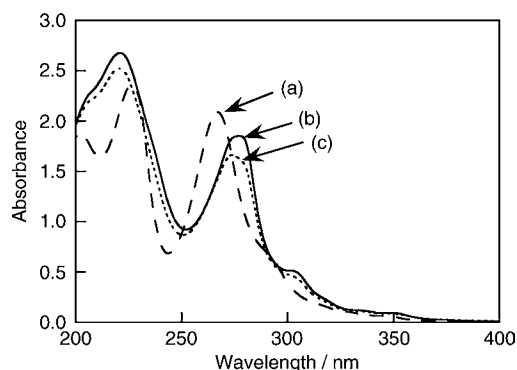
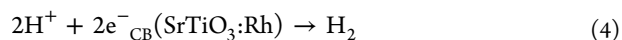
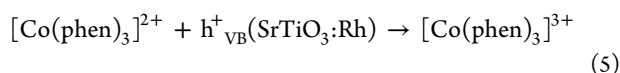


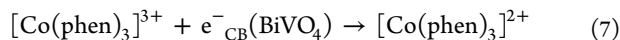
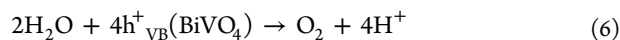
Figure 6. Absorption spectra of aqueous [Co(phen)₃]Cl₂ solutions (0.03 mmol L⁻¹) (a) before photocatalytic reaction, (b) after H₂ evolution on Ru/SrTiO₃:Rh photocatalyst, and (c) after overall water splitting by a (Ru/SrTiO₃:Rh)–(BiVO₄)–([Co(phen)₃]^{3+/2+}) system under visible light irradiation. Optical path length: 1 cm.

visible light irradiation accompanied with following reactions (eqs 4 and 5).





Moreover, when combined with BiVO_4 , overall water splitting proceeded (entry 6 in Table 2), meaning that the following reactions (eqs 6 and 7) proceeded on BiVO_4 .



As seen in eqs 5 and 7, $[\text{Co}(\text{phen})_3]^{3+/2+}$ works as an electron mediator over and over again. This was also supported by the larger turnover number than unity estimated from the reacted electrons to $[\text{Co}(\text{phen})_3]^{3+/2+}$ ions and the steady profile of water splitting for a long time as shown in Figure 2b. The absorption spectrum of the reactant solution after overall water splitting using the Z-scheme system (Figure 6c) indicates that the ratio of $[\text{Co}(\text{phen})_3]^{2+}$ to $[\text{Co}(\text{phen})_3]^{3+}$ was almost 1 to 9, revealing that the major valence of Co-complex was trivalent during photocatalytic water splitting. A $[\text{Co}(\text{bpy})_3]^{3+/2+}$ redox couple should also work similarly to $[\text{Co}(\text{phen})_3]^{3+/2+}$ during overall water splitting.

To know the redox potential of these Co-complexes, the electrochemical measurement was conducted. Current–potential curves of the aqueous $[\text{Co}(\text{bpy})_3]\text{SO}_4$, $[\text{Co}(\text{phen})_3]\text{Cl}_2$, and CoSO_4 solutions were shown in Figure 7. In the case of

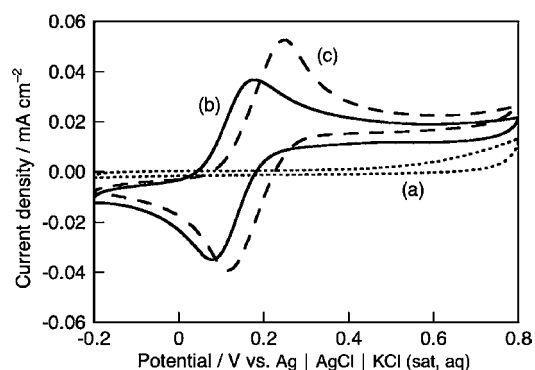


Figure 7. Current–potential curves of aqueous (a) CoSO_4 , (b) $[\text{Co}(\text{bpy})_3]\text{SO}_4$, and (c) $[\text{Co}(\text{phen})_3]\text{Cl}_2$ solutions. Working and counter electrodes: Pt plate (1 cm^2), reference: $\text{Ag} | \text{AgCl} | \text{KCl}$ (sat., aq), electrolyte: 50 mmol L^{-1} of an aqueous K_2SO_4 solution containing cobalt complexes (1 mmol L^{-1} each).

CoSO_4 solution, only a weak oxidation wave was observed, as shown in Figure 7a. In contrast, redox waves were observed for aqueous $[\text{Co}(\text{bpy})_3]\text{SO}_4$ and $[\text{Co}(\text{phen})_3]\text{Cl}_2$ solutions, as shown in Figure 7b and c. These waves were assigned to $[\text{Co}(\text{bpy})_3]^{3+/2+}$ and $[\text{Co}(\text{phen})_3]^{3+/2+}$ redox, and their redox potentials were 0.12 and 0.18 V vs $\text{Ag} | \text{AgCl} | \text{KCl}$ (sat., aq) under neutral pH conditions, respectively. These values agreed well with the values in the previous report.⁴² The redox potentials of the Co-complexes were suitably located between the electron donor level of $\text{SrTiO}_3:\text{Rh}$ ¹⁶ and the conduction band of BiVO_4 .^{14,43} Thus, it is thermodynamically possible that the $[\text{Co}(\text{bpy})_3]^{3+/2+}$ and $[\text{Co}(\text{phen})_3]^{3+/2+}$ electron mediators can shuttle between $\text{SrTiO}_3:\text{Rh}$ and BiVO_4 photocatalysts.

3.5. Inhibition Reactions in the Z-Scheme Photocatalyst Systems. The reactions (eqs 3 and 8) would also proceed during the water splitting because of the reversibility of the oxidation state of Co-complexes.



These reactions inhibit H_2 and O_2 evolution on $\text{Ru}/\text{SrTiO}_3:\text{Rh}$ and BiVO_4 , respectively. Therefore, we investigated these inhibition reactions as shown in Table 4. In the case of H_2

Table 4. Effects of an Inhibitor (Co(II)- or Co(III)-Complex Ion) on H_2 Evolution on $\text{Ru}/\text{SrTiO}_3:\text{Rh}$ and O_2 Evolution on BiVO_4 ^a

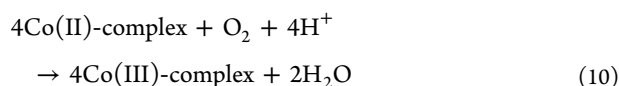
entry	photocatalyst	ligand	initial conc. of Co-complex / mmol L^{-1}		initial pH	initial activity / $\mu\text{mol h}^{-1}$	
			Co(II)	Co(III)		H_2	O_2
1	$\text{Ru}/\text{SrTiO}_3:\text{Rh}$	bpy	1	0	6.8	29	–
2	$\text{Ru}/\text{SrTiO}_3:\text{Rh}$	bpy	0.5	0.5	6.8	25	–
3	$\text{Ru}/\text{SrTiO}_3:\text{Rh}$	bpy	1	0	3.8	103	–
4	$\text{Ru}/\text{SrTiO}_3:\text{Rh}$	bpy	0.5	0.5	3.8	97	–
5	$\text{Ru}/\text{SrTiO}_3:\text{Rh}$	bpy	0.5	0	3.8	100	–
6	$\text{Ru}/\text{SrTiO}_3:\text{Rh}$	phen	1	0	6.8	26	–
7	$\text{Ru}/\text{SrTiO}_3:\text{Rh}$	phen	0.5	0.5	6.8	20	–
8	BiVO_4	bpy	0	0.5	6.8	–	8.6
9	BiVO_4	bpy	0.25	0.25	6.8	–	6.6
10	BiVO_4	bpy	0	0.5	3.8	–	3.0
11	BiVO_4	bpy	0.25	0.25	3.8	–	0.4
12	BiVO_4	bpy	0	0.25	3.8	–	2.3
13	BiVO_4	phen	0	0.5	6.8	–	8.3
14	BiVO_4	phen	0.25	0.25	6.8	–	2.4

^aReaction conditions: catalyst, 0.1 g; starting reactant solution, 120 mL of aqueous cobalt complex solution; light source, a 300-W Xe-arc lamp with a cutoff filter ($\lambda > 420 \text{ nm}$); cell, top-irradiation type. $\text{SrTiO}_3:\text{Rh}$ powder was prepared by calcination at 1373 K with Sr 3% excess.

evolution from an aqueous solution containing $[\text{Co}(\text{bpy})_3]^{2+}$ or $[\text{Co}(\text{phen})_3]^{2+}$ as an electron donor on the $\text{Ru}/\text{SrTiO}_3:\text{Rh}$ photocatalyst, no decreases in photocatalytic activities at the initial stage under acidic and neutral pH conditions were observed even if $[\text{Co}(\text{bpy})_3]^{3+}$ or $[\text{Co}(\text{phen})_3]^{3+}$ was added (entries 1–5 in Table 4). This result indicates that the inhibition reaction on $\text{Ru}/\text{SrTiO}_3:\text{Rh}$ (eq 3) was negligible. The poor effect of the inhibition reaction was also supported by the time course of H_2 evolution shown in Figure S1 (SI) and absorption spectra shown in Figure 6. These data indicate that all Co(II)-complex ions were consumed to form Co(III)-complex ions. In contrast, O_2 evolution from an aqueous solution containing $[\text{Co}(\text{bpy})_3]^{3+}$ or $[\text{Co}(\text{phen})_3]^{3+}$ as an electron acceptor on BiVO_4 was significantly suppressed by the addition of $[\text{Co}(\text{bpy})_3]^{2+}$ or $[\text{Co}(\text{phen})_3]^{2+}$ (entries 8–11, 13, and 14 in Table 4). If all dissolved Co(II)-complex ions were used for O_2 evolution on the BiVO_4 photocatalyst, $15 \mu\text{mol}$ and $7.75 \mu\text{mol}$ of O_2 should be obtained for entries 8, 10, and 13 and for entries 9, 11, 12, and 14, respectively. However, the O_2 evolution stopped before reaching those values, as shown in Figure S4 (SI). On the other hand, the concentration of the reactant of the Co(III)-complex ion did not significantly affect the activity (entries 10 and 12). The decrease in the activity for O_2 evolution by adding Co(II)-complexes indicates that the inhibition reaction 8 proceeded on BiVO_4 . The degree of the

decrease in the activity by addition of Co(II)-complex ions was small in the $[\text{Co}(\text{bpy})_3]^{3+}$ system in comparison with the $[\text{Co}(\text{phen})_3]^{3+}$ system (entries 8, 9, 13, and 14). The result indicates that the inhibition reaction 8 was suppressed in the $[\text{Co}(\text{bpy})_3]^{3+/2+}$ redox system resulting in that the activity of water splitting using the $[\text{Co}(\text{bpy})_3]^{3+/2+}$ redox system was higher than that using the $[\text{Co}(\text{phen})_3]^{3+/2+}$ redox system (Table 2). Moreover, the inhibition reaction was suppressed by controlling pH (entries 8–11).

Backward reactions such as water formation from evolved H_2 and O_2 (eq 9) and oxidation of Co(II)-complex ions by evolved O_2 (eq 10) were also possible to inhibit photocatalytic overall water splitting.



Water formation (eq 9) was examined by monitoring the pressures of H_2 (40 Torr) and O_2 (20 Torr) initially introduced into the photocatalyst reactor containing Ru/SrTiO₃:Rh and BiVO₄ suspended in the aqueous Co-complex solution in the dark. No decreases in the pressures of these gases were observed, indicating no water formation from H_2 and O_2 gases.

Oxidation of Co(II)-complex ions by O_2 (eq 10) was also examined by evaluating the photocatalytic activity of the Z-scheme system in the presence of 8 Torr of O_2 that was introduced before starting the reaction. The effect of introduction of an O_2 gas on the photocatalytic activity was not observed at all, indicating that the oxidation of the Co(II)-complex ions by O_2 was negligible.

3.6. Effect of pH on the Photocatalytic Activity for Overall Water Splitting. Figure 8 shows dependence of the photocatalytic activity for overall water splitting by the (Ru/SrTiO₃:Rh)–(BiVO₄)–($[\text{Co}(\text{bpy})_3]^{3+/2+}$) system on pH. The pH after overall water splitting is also shown on the second horizontal axis in Figure 8, because pH increased during the photocatalytic reaction at the initial stage by consumption of H^+ accompanied with excessive H_2 evolution and Co(III)-

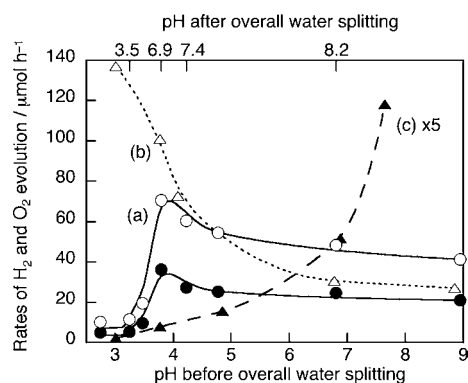


Figure 8. Effect of pH on photocatalytic activities for (a) overall water splitting by a (Ru/SrTiO₃:Rh)–(BiVO₄)–($[\text{Co}(\text{bpy})_3]^{3+/2+}$) system, (b) H_2 evolution over Ru/SrTiO₃:Rh photocatalyst, and (c) O_2 evolution over BiVO₄ photocatalyst. Reaction conditions: catalyst, 0.1 g each; starting reactant solution: (a,c) 0.5 mmol L⁻¹ and (b) 1 mmol L⁻¹ of aqueous $[\text{Co}(\text{bpy})_3]\text{SO}_4$ solutions (120 mL); light source: a 300 W Xe-arc lamp with a cutoff filter ($\lambda > 420$ nm). SrTiO₃:Rh powder was prepared by calcination at 1373 K with Sr 3% excess.

complex accumulation. The water splitting activity depended on pH. The highest activity was obtained around neutral pH after the reaction. Additionally, the similar activity was obtained by using a phosphate buffer to adjust the initial pH to 6.9, and no pH change was observed during reaction. These results indicate that the best pH during the photocatalytic reaction was not 3.8 but 6.9. The H_2 evolution on Ru/SrTiO₃:Rh and O_2 evolution on BiVO₄ from aqueous solutions containing $[\text{Co}(\text{bpy})_3]^{2+}$ and $[\text{Co}(\text{bpy})_3]^{3+}$ ions also depended on pH (Figure 8b and c). High H_2 evolution activity was obtained under acidic condition, whereas high O_2 evolution activity was obtained under basic condition.

The relationship between pH and photocatalytic activities can be explained using an energy diagram of the Z-scheme photocatalyst system as shown in Figure 9. The bottom of conduction band of SrTiO₃:Rh is 0.2 eV more negative than the redox potential of H^+/H_2 , and the impurity level formed by Rh³⁺ doped in SrTiO₃ is 2.4 eV more positive than the bottom of the conduction band.¹⁶ The bottom of the conduction band of BiVO₄ is almost equal to the redox potential of H^+/H_2 , and the top of the valence band is 2.4 eV more positive than the bottom of the conduction band.^{14,43} Since a band-level of an oxide semiconductor shifts with pH as well as the redox potential of H^+/H_2 and $\text{O}_2/\text{H}_2\text{O}$, the relative position between them does not change at any pH.^{44,45} In contrast, electrochemical measurements revealed that the redox potential of $[\text{Co}(\text{bpy})_3]^{3+/2+}$ was independent of pH. Lower pH of the reactant solution gave more positive shift of the band-level of SrTiO₃:Rh, resulting in that photogenerated holes at the impurity level in SrTiO₃:Rh possessed the larger driving force for oxidation of $[\text{Co}(\text{bpy})_3]^{2+}$ ions. Therefore, higher activity for H_2 evolution was obtained at lower pH as shown in Figure 8. In contrast, the photogenerated electrons in the conduction band of BiVO₄ had the smaller driving force for reduction of the $[\text{Co}(\text{bpy})_3]^{3+}$ ions under acidic conduction. In addition, the inhibition reaction 8 on BiVO₄ proceeded more easily under acidic condition than neutral pH condition as shown at entries 8–11 in Table 4. These factors accounted for the dependence of O_2 evolution over BiVO₄ on pH. The ratios of $[\text{Co}(\text{bpy})_3]^{2+}/[\text{Co}(\text{bpy})_3]^{3+}$ in basic, neutral, and acidic aqueous solutions during steadily photocatalytic water splitting were 4.5/5.5, 1.5/8.5, and 0.5/9.5, respectively. This difference in the ratios would attribute to the balance between reduction of $[\text{Co}(\text{bpy})_3]^{3+}$ on BiVO₄ and oxidation of $[\text{Co}(\text{bpy})_3]^{2+}$ on Ru/SrTiO₃:Rh and BiVO₄ under each pH condition. Thus, the activity for overall water splitting showed volcano-type dependence on pH, so that the highest activity was obtained around neutral pH.

4. CONCLUSIONS

$[\text{Co}(\text{bpy})_3]^{3+/2+}$ and $[\text{Co}(\text{phen})_3]^{3+/2+}$ redox couples were utilized as an electron mediator for visible-light-driven Z-scheme photocatalyst systems. These systems with Ru/SrTiO₃:Rh as a H_2 -evolving photocatalyst and BiVO₄ as an O_2 -evolving photocatalyst suspended in the aqueous Co-complex solutions split water into H_2 and O_2 in a stoichiometric amount under visible light irradiation. The activity of the (Ru/SrTiO₃:Rh)–(BiVO₄)–($[\text{Co}(\text{bpy})_3]^{3+/2+}$) system depended on pH of the reactant solution, and the highest activity was obtained under neutral pH. Moreover, the inhibition reaction against O_2 evolution by the oxidation of Co(II)-complex ions on BiVO₄ was remarkable under acidic condition but was suppressed under neutral condition. In

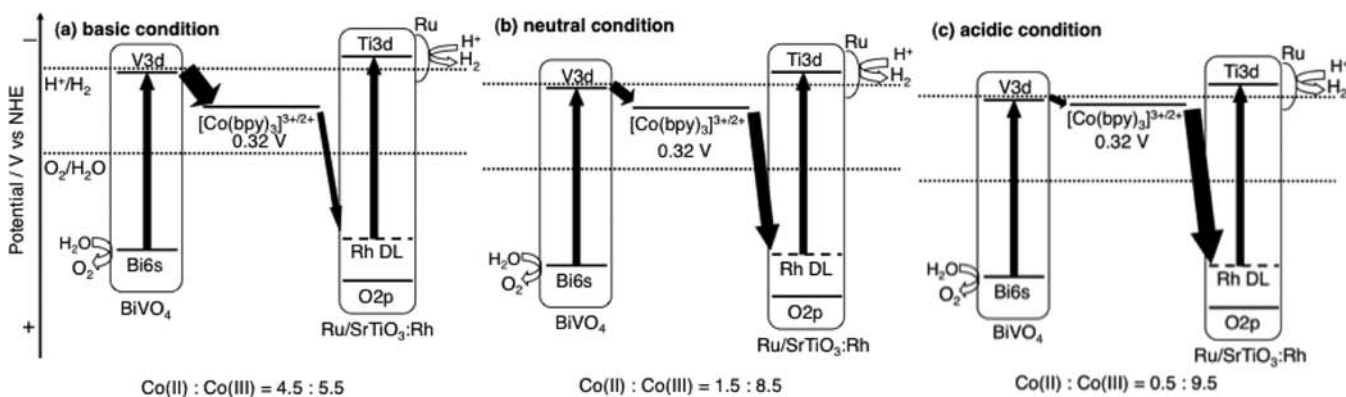


Figure 9. Energy diagrams of the Z-scheme photocatalyst system, (Ru/SrTiO₃:Rh)–(BiVO₄)–([Co(bpy)₃]^{3+/2+}), and the ratio of [Co(bpy)₃]²⁺ ions to [Co(bpy)₃]³⁺ ions during overall water splitting under basic, neutral, and acidic conditions.

contrast, the inhibition reaction against H₂ evolution by the reduction of Co(III)-complex ions on Ru/SrTiO₃:Rh was negligible regardless of pH. The (Ru/SrTiO₃:Rh)–(BiVO₄)–([Co(bpy)₃]^{3+/2+}) system was confirmed to be active for solar water splitting. Moreover, separated evolution of H₂ from O₂ by water splitting under visible light irradiation was demonstrated by using the (Ru/SrTiO₃:Rh)–(BiVO₄)–([Co(bpy)₃]^{3+/2+}) system. Thus, we succeeded in development of the new and attractive Z-scheme photocatalyst system.

■ ASSOCIATED CONTENT

Supporting Information

H₂ evolution on Ru/SrTiO₃:Rh from an aqueous solution containing Co(II)-complex ions under visible light irradiation, H₂ and O₂ evolution under visible light irradiation by a (Ru/SrTiO₃:Rh)–(WO₃) system with tris-(bipyridyl)cobalt complex, XRD patterns of SrTiO₃:Rh prepared with Sr excess, and O₂ evolution on BiVO₄ from an aqueous solution containing Co(III)-complex ions under visible light irradiation. This material is available free of charge via the Internet at <http://pubs.acs.org>.

■ AUTHOR INFORMATION

Corresponding Author

a-kudo@rs.kagu.tus.ac.jp

Present Address

[†]Institute of Multidisciplinary Research for Advanced Materials, Tohoku University, Japan.

Notes

The authors declare no competing financial interest.

■ ACKNOWLEDGMENTS

We gratefully thank Mr. Nemoto for the assistance of solar water splitting, and Dr. Saito and Dr. Iwase for useful discussion. This work was supported by a Grant-in-Aid (No. 24107004) for Scientific Research on Innovative Areas (No. 2406) from the Ministry of Education, Culture, Sports, Science & Technology in Japan.

■ REFERENCES

- (1) Sato, S.; White, J. M. *Chem. Phys. Lett.* **1980**, *72*, 83.
- (2) Lehn, J.-M.; Sauvage, J.-P.; Ziessel, R. *Nouv. J. Chim.* **1980**, *4*, 623.
- (3) Kato, H.; Kudo, A. *Catal. Lett.* **1999**, *58*, 153.
- (4) Arakawa, H.; Sayama, K. *Catal. Surv. Jpn.* **2000**, *4*, 75.
- (5) Kato, H.; Kudo, A. *J. Phys. Chem. B* **2001**, *105*, 4285.
- (6) Maeda, K.; Domen, K. *J. Phys. Chem. C* **2007**, *111*, 7851.
- (7) Osterloh, F. E. *Chem. Mater.* **2008**, *20*, 35.
- (8) Kudo, A.; Miseki, Y. *Chem. Soc. Rev.* **2009**, *38*, 253.
- (9) Inoue, Y. *Energy Environ. Sci.* **2009**, *2*, 364.
- (10) Kato, H.; Asakura, K.; Kudo, A. *J. Am. Chem. Soc.* **2003**, *125*, 3082.
- (11) Maeda, K.; Teramura, K.; Lu, D.; Takata, T.; Saito, N.; Inoue, Y.; Domen, K. *Nature* **2006**, *440*, 295.
- (12) Lee, Y.; Teramura, K.; Hara, M.; Domen, K. *Chem. Mater.* **2007**, *19*, 2120.
- (13) Darwent, J. R.; Mills, A. *J. Chem. Soc., Faraday Trans. 2* **1982**, *78*, 359.
- (14) Kudo, A.; Omori, K.; Kato, H. *J. Am. Chem. Soc.* **1999**, *121*, 11459.
- (15) Ishii, T.; Kato, H.; Kudo, A. *J. Photochem. Photobiol., A* **2004**, *163*, 181.
- (16) Konta, R.; Ishii, T.; Kato, H.; Kudo, A. *J. Phys. Chem. B* **2004**, *108*, 8992.
- (17) Shimodaira, Y.; Kato, H.; Kobayashi, H.; Kudo, A. *J. Phys. Chem. B* **2006**, *110*, 17790.
- (18) Park, H.; Choi, W. *Langmuir* **2006**, *22*, 2906.
- (19) Mau, A. W.; Huang, C.; Kakuta, N.; Bard, A. J.; Campion, A.; Fox, M. A.; White, J. M.; Webber, A. E. *J. Am. Chem. Soc.* **1984**, *106*, 6537.
- (20) Ishikawa, A.; Takata, T.; Kondo, J. N.; Hara, M.; Kobayashi, H.; Domen, K. *J. Am. Chem. Soc.* **2002**, *124*, 13547.
- (21) Tsuji, I.; Kato, H.; Kudo, A. *Angew. Chem., Int. Ed.* **2005**, *44*, 3565.
- (22) Yamashita, D.; Takata, T.; Hara, M.; Kondo, J. N.; Domen, K. *Solid State Ionics* **2004**, *172*, 591.
- (23) Hisatomi, T.; Hasegawa, K.; Teramura, K.; Takata, T.; Hara, M.; Domen, K. *Chem. Lett.* **2007**, *36*, 558.
- (24) Fujihara, K.; Ohno, T.; Matsumura, M. *J. Chem. Soc., Faraday Trans.* **1998**, *94*, 3705.
- (25) Sayama, K.; Mukasa, K.; Abe, R.; Abe, Y.; Arakawa, H. *Chem. Commun.* **2001**, 2416.
- (26) Abe, R.; Takata, T.; Sugihara, H.; Domen, K. *Chem. Commun.* **2005**, 3829.
- (27) Kato, H.; Sasaki, Y.; Iwase, A.; Kudo, A. *Bull. Chem. Soc. Jpn.* **2007**, *80*, 2457.
- (28) Higashi, M.; et al. *Chem. Lett.* **2008**, *37*, 138.
- (29) Sasaki, Y.; Iwase, A.; Kato, H.; Kudo, A. *J. Catal.* **2008**, *259*, 133.
- (30) Abe, R.; Shinmei, K.; Hara, K.; Ohtani, B. *Chem. Commun.* **2009**, 3577.
- (31) Sasaki, Y.; Nemoto, H.; Saito, K.; Kudo, A. *J. Phys. Chem. C* **2009**, *113*, 17536.
- (32) Bae, S. W.; Ji, A. M.; Hong, S. J.; Jang, J. M.; Lee, J. S. *Int. J. Hydrogen Energy* **2009**, *34*, 3243.
- (33) Nusbaumer, H.; Moser, J.; Zakeeruddin, S. M.; Nazeeruddin, M. K.; Grätzel, M. *J. Phys. Chem. B* **2001**, *105*, 10461.
- (34) Sapp, S. A.; Elliot, C. M.; Contado, C.; Caramori, S.; Bignozzi, C. A. *J. Am. Chem. Soc.* **2002**, *124*, 11215.

- (35) Nusbaumer, H.; Zakeeruddin, S. M.; Moser, J.; Grätzel, M. *Chem.—Eur. J.* **2003**, *9*, 3756.
- (36) Nakada, S.; Makimoto, Y.; Kubo, W.; Kitamura, T.; Wada, Y.; Yanagida, S. *J. Phys. Chem. B* **2005**, *109*, 3488.
- (37) Hosogi, Y.; Tanabe, K.; Kato, H.; Kobayashi, H.; Kudo, A. *Chem. Lett.* **2004**, *33*, 28.
- (38) Kato, H.; Kudo, A. *J. Phys. Chem. B* **2002**, *106*, 5029.
- (39) Jager, F. M.; Dijk, J. A. *Z. Anorg. Allg. Chem.* **1936**, *227*, 273.
- (40) Yamasaki, K.; Hara, T.; Yasuda, M. *Proc. Jpn. Acad.* **1953**, *29*, 337.
- (41) Simic, M. G.; Hoffman, M. Z.; Cheney, R. P.; Mulazzani, Q. G. *J. Phys. Chem.* **1979**, *83*, 439.
- (42) Krishnan, C. V.; Brunshwig, B. S.; Creutz, C.; Sutin, N. *J. Am. Chem. Soc.* **1985**, *107*, 2005.
- (43) Oshikiri, M.; Boero, M.; Ye, J.; Zou, Z.; Kido, G. *J. Chem. Phys.* **2002**, *117*, 7313.
- (44) Nozik, J. *Annu. Rev. Phys. Chem.* **1978**, *29*, 189.
- (45) Duonghong, D.; Ramsden, J.; Grätzel, M. *J. Am. Chem. Soc.* **1982**, *104*, 2977.